Supporting Information

Synthesis of Radiolabelled Aryl Azides from Diazonium Salts: Experimental and Computational Results Permit to Identify the Preferred Mechanism

Sameer M. Joshi,[a] Abel de Cózar,[b,c,d,e] Vanessa Gómez-Vallejo,[f] Jacek Koziorowski,[g] Jordi Llop,[a,] and Fernando P. Cossío[b,d,e*].*

jllop@cicbiomagune.es, fp.cossio@ehu.es

[a] *Radiochemistry and Nuclear Imaging, CIC biomaGUNE, Paseo Miramón 182, Parque Tecnológico de San Sebastián, 20009 San Sebastián/Donostia, Spain.*
[b] *Departamento de Química Orgánica I, Facultad de Química, Universidad del País Vasco/Euskal Herriko Unibertsitatea (UPV/EHU), 20018 San Sebastián/Donostia, Spain.*
[c] *Ikerbasque, Basque Foundation for Science, 48018, Bilbao, Spain.*
[d] *Centro de Innovación en Química Avanzada (ORFEO-CINQA).*
[e] *Donostia International Physics Center (DIPC), 20018, San Sebastián/Donostia, Spain.*
[f] *Radiochemistry Platform, CIC biomaGUNE, Paseo Miramón 182, Parque Tecnológico de San Sebastián, 20009, San Sebastián/Donostia, Spain.*
[g] *Department of Radiation Physics and Department of Medical and Health Sciences, Linköping University, Linköping, Sweden.*

CONTENTS

General Information

Aniline (reagent plus grade 99%), sodium nitrite (ACS reagent, 97%), acetic acid (Reagentplus®, >99%), hydrazine hydrate solution (iodometric, 78-82%), and azidobenzene solution (0.5 M in tert-butyl methyl ether, >95%) were purchased from Sigma-Aldrich and used without further purification. Hydrochloric acid (37%, extrapure, Ph. Eur.) and dichloromethane (synthesis grade) were purchased from Scharlau. Ultrapure water (Type I water, ISO 3696) was obtained from a Milli-Q® system (Merck Millipore).

Synthesis of ^{13}N-labelled phenylazide (Route B in Scheme 1)

Nitrogen-13 (30 mCi, 1110 GBq) was produced in an IBA Cyclone 18/9 cyclotron by irradiation of purified water *via* the $^{16}O(p,\alpha)^{13}N$ nuclear reaction. The irradiated solution was passed through a glass column filled with pre-treated cadmium[1] to quantitatively reduce $[^{13}N]NO_3^-$ into $[^{13}N]NO_2^-$. A sample of this solution (20 µL) was analyzed by HPLC to confirm quantitative reduction of $[^{13}N]NO_3^-$ into $[^{13}N]NO_2^-$, using an Agilent 1200 series HPLC equipped with a quaternary pump, a multiple wavelength detector and a radiometric detector (Gabi, Raytest). An HP Asahipak ODP-50 (5 µm, 125x4 mm, Teknokroma, Spain) was used as stationary phase, and a solution containing additive for ionic chromatography (15 mL) in a mixture water/acetonitrile (86/14, V = 1L) basified to pH = 8.6 with 1M sodium hydroxide solution was used as the mobile phase at a flow rate of 1 mL/min. Simultaneous UV (λ = 254 nm) and isotopic detection were used.

The solution containing $[^{13}N]NO_2^-$ was added drop-wise to a second solution containing aniline (23mg, 0.25 mmole) in HCl (0.1mL of 37% HCl in 0.15mL water). The reaction for the formation of the diazonium salt was allowed to occur (1 minute, RT). In a separate vial, a mixture of sodium nitrite solution (17mg in 0.1mL water, 0.25 mmole), acetic acid (120 µL, 1.98 mmole) and hydrazine hydrate solution (70 µL, 1.41 mmole) was prepared and added drop-wise to the previous solution (total addition time 1 min, and the reaction for the formation of ^{13}N-labelled azide was allowed to occur for 1 min. The activity (A_1) was measured in a dose calibrator (PETDOSE HC, Comecer), the vial was flushed with nitrogen gas (1 minute) and the activity was measured again (A_2). The amount of $[^{13}N]N_2$ was calculated as A_2-A_1. The reaction crude was analyzed by HPLC using an Agilent 1200 Series HPLC system with a multiple wavelength UV detector (λ = 254 nm) and a radiometric detector (Gabi, Raytest). A RP-C18 column (Mediterranean Sea18, 4.6x250 mm, 5 µm particle size) was used as stationary phase and ammonium formate (pH = 3.9) (A)/methanol (B) was used as the mobile phase. The following gradient was used: t=0 min, 90%A/10%B; t=2 min, 90%A/10%B; t=4 min, 35%A/65%B; t=6 min, 20%A/80%B; t=12 min, 20%A/80%B; t=15 min, 90%A/10%B. The presence of the desired labelled specie was confirmed by co-elution with reference

[1] Cadmium (20 g., granular, 5-20 mesh) was introduced in a glass column (10 mm i.d., 8 cm in length) and sequentially washed with 1 M HCl (2 x 20 mL), distilled water (3 x 20 mL), 0.5 M aqueous $CuSO_4$ solution (2 x 20 mL), 0.1 M aqueous NH_4Cl solution (2 x 20 mL) and distilled water (3 x 20 mL).

standard (retention time = 9.6 min, see Figure S1). The amount of [^{13}N]phenylazide was determined as the product (A_2 x A_U), where A_U is the area under the peak for phenyl azide (radiometric detector, expressed as percentage with respect to all integrated peaks in the chromatogram). All radioactivity values were decay corrected to the same time point.

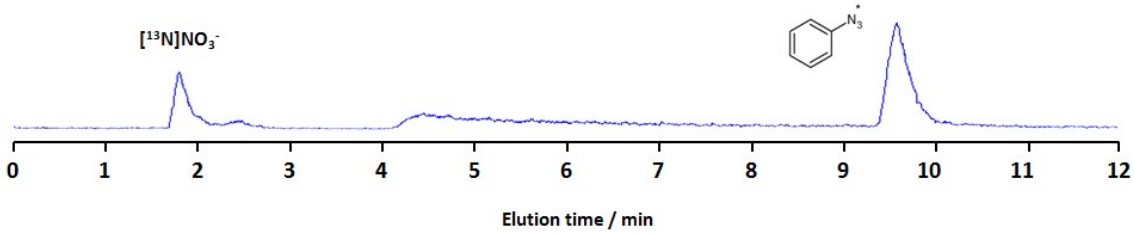

Figure S1: HPLC Chromatographic profile of the reaction mixture. The labelled azide appears at t=9.6 min.

Synthesis of ^{13}N-labelled phenylazide (Route A in Scheme 1)

[^{13}N]NO_2^- was prepared as mentioned in route B. The resulting solution was added drop-wise to a solution containing hydrazine hydrate solution (70 µL, 1.41 mmole) and acetic acid (120 µL, 1.98 mmole), and the reaction was allowed to occur (1 minute, RT). In a separate vial, a solution of aniline (23mg, 0.25 mmole) in HCl (0.1mL of 37% HCl in 0.15mL water) was reacted with sodium nitrite (17mg in 0.1mL water, 0.25 mmole) for 1 minute at RT to form the non-radioactive diazonium salt. The first solution was added drop wise to the second solution (total duration 1 minute) and the reaction was allowed to occur (1 min, RT). Sample processing, identification of the labelled species and determination of the amount of [^{13}N]N_2 and [^{13}N]phenyl azide was performed as in Route B.

Analysis of the radioactive gas

The synthesis of ^{13}N-labelled phenylazide was performed following the methodologies described above. However, before flushing the reaction vials with nitrogen gas, a sample of the gas from the sealed reaction vial was withdrawn and analyzed by radio-GC-MS. Analyses were performed on an Agilent 7820A network GC with an automatic loop injection system (loop volume = 250 µL) combined with an Agilent 5975c inert XL MSD with Triple axis detector. A J&W PoraPLOT column (length 27.5m, internal diameter 0.32 mm) was used as stationary phase. The inlet conditions were 150 °C, 25 psi and a flow rate of 3.5 mL/min using a 1:10 split injector with helium (99.9999%) as the carrier gas. The oven temperature was set to 36 °C. Total run time was 6 min (retention time = 1.45 min). Simultaneous detection using a radiometric detector (Gabi, raytest) and MS were used using a post-column split. MS was operated in scan mode in the range 10-150 Da.

Computational Results

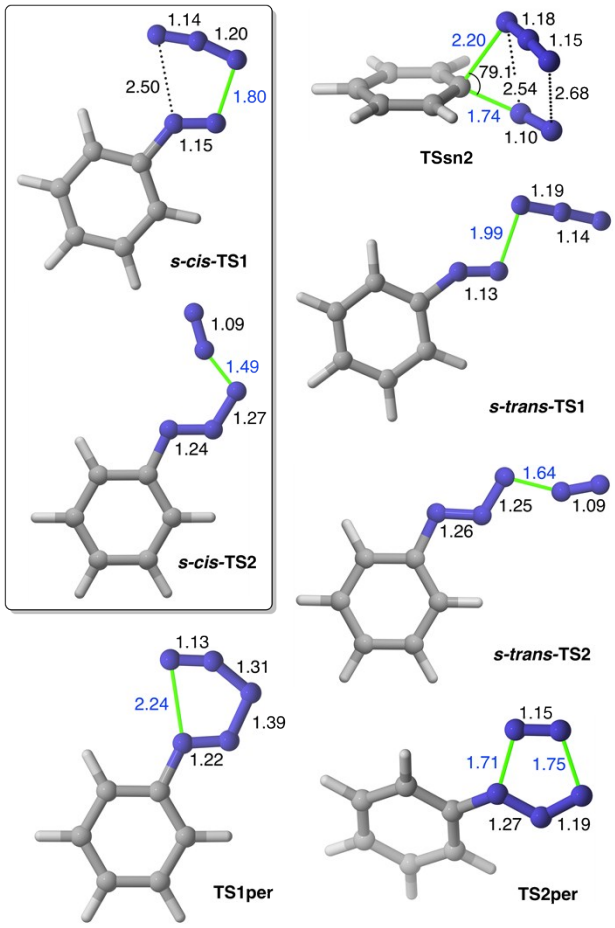

Figure S2. Chief geometric features (M06-2X/def2-TZVPP level of theory) of transition structures gathered in Figure 2 of the main text. Bond distances and angles are given in Å and deg., respectively.

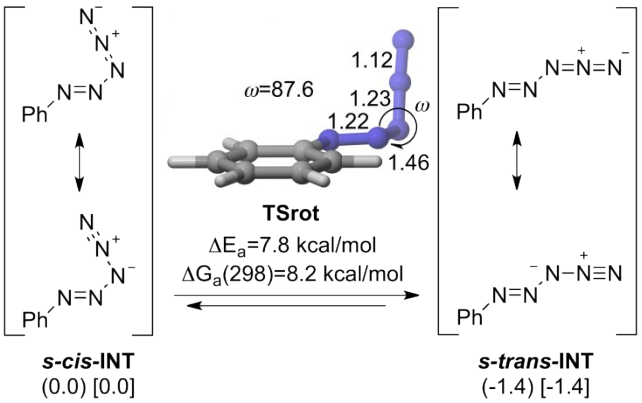

Figure S3. M06-2X(PCM)/def2-TXVPP relative energies (in kcal/mol, numbers in parentheses) and relative Gibbs energies (at 298 K, in kcal/mol, numbers in square brackets) of zwitterionic intermediates ***s-cis***- and ***s-trans*-INT**. The main geometric features and activation energies of transition structure **TSrot** that connects both conformers are also indicated. Bond distances and angles are given in Å and deg., respectively. Dihedral angle ω describes the torsion about the N2-N3 bond.

Kinetic Simulations

Since the ensemble of alternative reaction paths gives rise to a complex mechanistic scheme, we performed numeric kinetic simulations in order to evaluate the impact of each possible mechanism on the formation of phenylazide **2** at 298 K. First, we computed the kinetic constants associated with each elementary step from the corresponding free energy values reported in Table S1 according to the Eyring equation ($k_i=(k_bT/h)\exp[-\Delta G_a/RT]$). These values are gathered in Table S2. The notation used for the different kinetic constants is that indicated in Figure S4.

Table S1. Total electronic energies[a] (E, in a.u.), zero point correction of energy[b] (ZPCE, in a.u.), thermal corrections to Gibbs free energies[b] (TCGE, in a. u.) and number of imaginary frequencies[c] (NIMAG) of all stationary points discussed in the main text.

Structure	E	ZPCE	TCGE	NIMAG(ν)
1	-340.909241	0.100227	0.069959	0
N_3^-	-164.331227	0.011302	-0.009852	0
RC	-505.256076	0.112680	0.076092	0
***s-cis*-INT1**	-505.264761	0.113499	0.077939	0
***s-trans*-INT1**	-505.267179	0.113810	0.078329	0
INTper	-505.320504	0.117115	0.082928	0
2+N_2	-505. 666837	0.111213	0.070915	0
2	-395.829422	0.104537	0.072625	0
N_2	-109.536273	0.005741	-0.012675	0
***s-cis*-TS1**	-505.248494	0.112217	0.077531	1 (-171.8042)
***s-trans*-TS1**	-505. 234044	0.111455	0.075186	1 (-235.5360)
***s-cis*-TS2**	-505.255313	0.111201	0.075298	1 (-752.6364)
***s-trans*-TS2**	-505.231858	0.110073	0.074182	1 (-708.9640)
TSrot	-505.252342	0.113447	0.078639	1 (-152.8671)
TSsn2	-505.216889	0.109043	0.073751	1 (-554.9892)
TS1per	-505.253207	0.112444	0.078048	1 (-323.7562)
TS2per	-505.272447	0.112528	0.078006	1 (-646.9926)

[a]Computed at the M06-2X(PCM)/def2-TZVPP level of theory. [b]Computed at 298 K at the M06-2X(PCM)/def2-TZVPP level of theory. [c]When NIMAG=1, the imaginary frequency ν (in parentheses) is given in cm^{-1}.

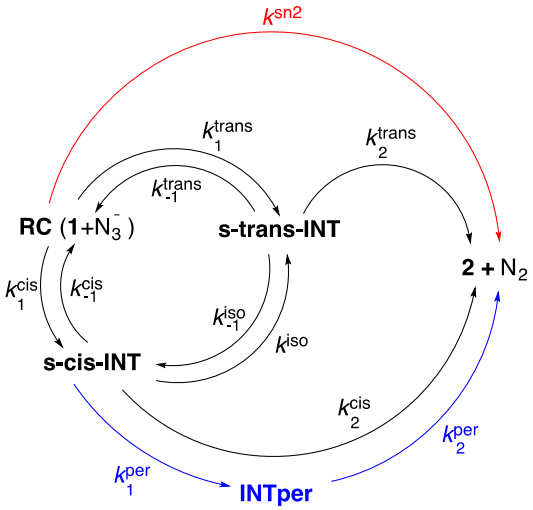

Figure S4. Kinetic scheme and kinetic rate constants associated with the elementary steps corresponding to the **1**+N_3^- → **2**+N_2 reaction.

Table S2. Calculated kinetic constants[a] (k_i^a, s^{-1}) associated with the formation of **2** computed using Eyring equation and the corresponding Gibbs free energy barriers.

Elementary step	k_i^a	Value
RC (**1**+N_3^-) → **2**+N_2	k^{sn2}	8.4 x 10^{-8}
RC (**1**+N_3^-) → *s-trans*-**INT**	k_1^{trans}	1.3 x 10^{3}
s-trans-**INT** → **RC** (**1**+N_3^-)	k_{-1}^{trans}	8.6 x 10^{-2}
RC (**1**+N_3^-) → *s-cis*-**INT**	k_1^{cis}	4.1 x 10^{8}
s-cis-**INT** → **RC** (**1**+N_3^-)	k_{-1}^{cis}	2.9 x 10^{5}
s-trans-**INT** → **2**+N_2	k_2^{trans}	2.6 x 10^{-2}
s-cis-**INT** → **2**+N_2	k_2^{cis}	4.3 x 10^{9}
s-cis-**INT** → **INT**per	k_1^{per}	2.7 x 10^{7}
INTper → **2**+N_2	k_2^{per}	9.4 x 10^{5}
s-cis-**INT** → *s-trans*-**INT**	k^{iso}	6.6 x 10^{6}
s-trans-**INT** → *s-cis*-**INT**	k_{-1}^{iso}	6.3 x 10^{7}

[a]Values computed at 298.15 K.

According to the kinetic scheme gathered in Figures 2 and S4, formation of **2** from the corresponding reaction intermediates can be assumed as irreversible and therefore the total reaction rate can be described by the following equation:

$$rate = k^{sn2}\left[RC\right] + k_2^{cis}\left[scisINT\right] + k_2^{trans}\left[stransINT\right] + k_2^{per}\left[INTper\right] \quad (1)$$

The evolution of the different reaction intermediates can be described as indicated in equations (2)-(5):

$$\frac{d}{dt}\left[RC\right] = -\left(k^{sn2} + k_1^{cis} + k_1^{trans}\right)\left[RC\right] + k_{-1}^{cis}\left[scisINT\right] + k_{-1}^{trans}\left[stransINT\right] \quad (2)$$

$$\frac{d}{dt}\left[scisINT\right] = k_1^{cis}\left[RC\right] + k_{-1}^{iso}\left[stransINT\right] - \left(k_{-1}^{cis} + k^{iso} + k_1^{per} + k_2^{cis}\right)\left[scisINT\right] \quad (3)$$

$$\frac{d}{dt}\left[stransINT\right] = k_1^{trans}\left[RC\right] + k^{iso}\left[scisINT\right] - \left(k_{-1}^{cis} + k_{-1}^{iso} + k_2^{trans}\right)\left[stransINT\right] \quad (4)$$

$$\frac{d}{dt}\left[INTper\right] = k_1^{per}\left[scisINT\right] - k_2^{per}\left[INTper\right] \quad (5)$$

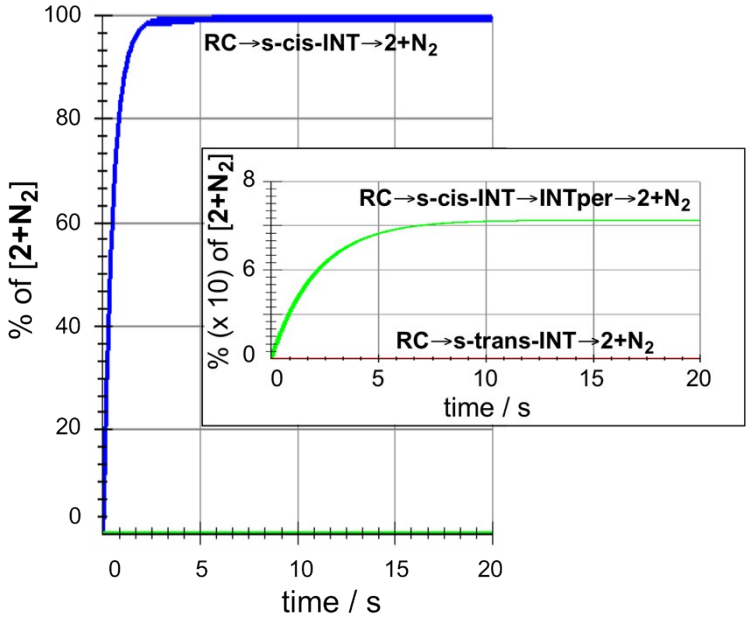

Figure S5. Simulated reaction outcome obtained by numerical integration of the previous kinetic equations using eqs. (1)-(5) and the rate constants collected in Table S2. The inset highlights the formation of **2** via **INTper**.

Numerical integration of equations (1)-(5) showed the quick stabilization of products **2**+N_2, as it is shown in Figure S5. Using these results, we were able to identify the contribution of the different reaction paths to the formation of phenylazide. As it can be seen by inspection of Figure S5, nearly all the reaction products **2** and N_2 stem from zwitterionic intermediate ***s-cis*-INT**. A careful analysis revealed the low but measurable contribution of five-membered intermediate **INTper** to the final outcome, which can be estimated as $0.72 \approx 1$ %, the contribution of zwitterionic route via ***s-cis*-INT** being therefore of ca. 99 %. Neither the direct S_N2 reaction nor the stepwise process via ***s-trans*-INT** (including the isomerization reaction) contributed significantly to the formation of reaction product **2**.

Cartesian coordinates (optimized at the M06-2X(PCM)/def2-TZVPP level) of all the stationary points discussed in the main text.

1

Center Number	Atomic Number	Atomic Type	Coordinates (Angstroms) X	Y	Z
1	6	0	0.547198	0.001774	0.001999
2	7	0	1.941521	0.000945	0.000148
3	6	0	-0.095581	1.235927	0.001920
4	6	0	-1.476229	1.212972	-0.000148
5	6	0	-2.155036	-0.001939	-0.002292
6	6	0	-1.473155	-1.215022	-0.000158
7	6	0	-0.092597	-1.233718	0.001943
8	7	0	3.030743	-0.000498	-0.002954
9	1	0	0.468220	2.156527	0.003431
10	1	0	-2.023186	2.143974	-0.000638
11	1	0	-3.235936	-0.003507	-0.005542
12	1	0	-2.017010	-2.147821	-0.000708
13	1	0	0.474462	-2.152263	0.003512

N_3^-

Center Number	Atomic Number	Atomic Type	Coordinates (Angstroms) X	Y	Z
1	7	0	0.000000	0.000000	0.000000
2	7	0	0.000000	0.000000	-1.167881
3	7	0	0.000000	0.000000	1.167881

RC

Center Number	Atomic Number	Atomic Type	Coordinates (Angstroms) X	Y	Z
1	6	0	0.541538	-0.265922	0.037324
2	7	0	-0.818474	-0.690728	0.080948
3	6	0	0.864591	1.076521	0.111707
4	6	0	2.209311	1.408857	0.079031
5	6	0	3.176004	0.417511	-0.031613
6	7	0	-1.571815	-1.501090	0.144431
7	7	0	-3.734721	-0.260247	-0.008356
8	6	0	2.815686	-0.923975	-0.106443
9	6	0	1.482519	-1.286377	-0.068638
10	7	0	-2.960817	0.599016	-0.082911
11	7	0	-2.069121	1.352753	-0.145637

12	1	0	0.082129	1.813369	0.190541
13	1	0	2.499870	2.447758	0.137514
14	1	0	4.221815	0.690798	-0.060192
15	1	0	3.572202	-1.690336	-0.194273
16	1	0	1.170738	-2.319205	-0.121115

***s-cis*-INT1**

Center Number	Atomic Number	Atomic Type	Coordinates (Angstroms) X	Y	Z
1	6	0	0.000000	0.598394	0.000000
2	7	0	0.112464	-0.820642	0.000000
3	6	0	1.205480	1.289145	0.000000
4	6	0	1.207441	2.677025	0.000000
5	6	0	0.005321	3.369584	0.000000
6	7	0	-0.955702	-1.431123	0.000000
7	7	0	-0.857250	-2.821287	0.000000
8	6	0	-1.200476	2.672885	0.000000
9	6	0	-1.211696	1.289038	0.000000
10	7	0	0.337828	-3.228361	0.000000
11	7	0	1.357841	-3.659571	0.000000
12	1	0	2.129113	0.726201	0.000000
13	1	0	2.145783	3.214304	0.000000
14	1	0	0.003126	4.451037	0.000000
15	1	0	-2.136434	3.214880	0.000000
16	1	0	-2.144281	0.744046	0.000000

***s-trans*-INT1**

Center Number	Atomic Number	Atomic Type	Coordinates (Angstroms) X	Y	Z
1	6	0	0.000000	0.856678	0.000000
2	7	0	-1.030652	-0.126277	0.000000
3	6	0	-0.438793	2.175205	0.000000
4	6	0	0.483344	3.212393	0.000000
5	6	0	1.841808	2.929772	0.000000
6	7	0	-0.627409	-1.287065	0.000000
7	7	0	-1.708876	-2.166999	0.000000
8	6	0	2.277887	1.607173	0.000000
9	6	0	1.365133	0.567395	0.000000
10	7	0	-1.267724	-3.340966	0.000000
11	7	0	-0.995849	-4.416461	0.000000
12	1	0	-1.502726	2.370109	0.000000
13	1	0	0.139853	4.237732	0.000000
14	1	0	2.562857	3.735919	0.000000
15	1	0	3.337154	1.388472	0.000000
16	1	0	1.700150	-0.459550	0.000000

INTper

Center Number	Atomic Number	Atomic Type	Coordinates (Angstroms) X	Y	Z
1	6	0	-0.386335	0.000002	0.000004
2	7	0	1.044196	-0.000005	0.000006
3	6	0	-1.054887	-1.214102	0.000527
4	6	0	-2.441072	-1.203234	0.000510
5	6	0	-3.134373	0.000000	0.000001
6	7	0	1.782453	1.082314	0.001142
7	7	0	2.999270	0.665263	0.000622
8	6	0	-2.441069	1.203233	-0.000506
9	6	0	-1.054883	1.214107	-0.000523
10	7	0	2.999261	-0.665258	-0.000588
11	7	0	1.782450	-1.082322	-0.001193
12	1	0	-0.502885	-2.141942	0.000987
13	1	0	-2.978238	-2.141195	0.000963
14	1	0	-4.215441	0.000006	-0.000002
15	1	0	-2.978236	2.141195	-0.000965
16	1	0	-0.502890	2.141952	-0.000980

2+N_2

Center Number	Atomic Number	Atomic Type	Coordinates (Angstroms) X	Y	Z
1	6	0	0.497408	-0.164416	-0.487241
2	7	0	-0.771697	-0.312123	-1.111936
3	6	0	1.365426	0.752078	-1.072997
4	6	0	2.622966	0.950123	-0.525505
5	6	0	3.020599	0.240300	0.602147
6	7	0	-1.549117	-1.106331	-0.587054
7	7	0	-2.323969	-1.798777	-0.178073
8	6	0	2.147675	-0.670994	1.181288
9	6	0	0.885037	-0.878263	0.643428
10	7	0	-3.344007	1.130310	0.916438
11	7	0	-2.616529	1.814269	0.489054
12	1	0	1.043721	1.296952	-1.950413
13	1	0	3.295676	1.662883	-0.983630
14	1	0	4.003188	0.396073	1.025938
15	1	0	2.446991	-1.228451	2.059073
16	1	0	0.212995	-1.591853	1.103307

2

Center Number	Atomic Number	Atomic Type	Coordinates (Angstroms) X	Y	Z
1	6	0	0.152349	-0.376347	0.000338
2	7	0	1.469412	-0.910821	0.000555
3	6	0	-0.126474	0.987524	0.000430
4	6	0	-1.447315	1.413272	0.000102
5	6	0	-2.486359	0.492618	-0.000276
6	6	0	-2.197422	-0.867401	-0.000303
7	6	0	-0.883361	-1.305576	0.000019
8	7	0	3.292619	0.561229	-0.000604
9	7	0	2.391348	-0.097679	-0.000181
10	1	0	0.676228	1.713886	0.000846
11	1	0	-1.661003	2.473648	0.000145
12	1	0	-3.512963	0.831692	-0.000549
13	1	0	-3.000030	-1.592576	-0.000607
14	1	0	-0.644405	-2.360286	-0.000085

N_2

Center Number	Atomic Number	Atomic Type	Coordinates (Angstroms) X	Y	Z
1	7	0	0.000000	0.000000	0.542886
2	7	0	0.000000	0.000000	-0.542886

***s-cis*-TS1**

Center Number	Atomic Number	Atomic Type	Coordinates (Angstroms) X	Y	Z
1	6	0	0.548118	-0.140868	0.000000
2	7	0	-0.868822	-0.293679	0.000000
3	6	0	1.029268	1.157384	0.000000
4	6	0	2.401795	1.355009	0.000000
5	6	0	3.257680	0.261578	0.000000
6	7	0	-1.520585	-1.245166	0.000000
7	7	0	-3.294866	-0.749919	0.000000
8	6	0	2.752455	-1.035996	0.000000
9	6	0	1.386004	-1.250654	0.000000
10	7	0	-3.119838	0.432935	0.000000
11	7	0	-2.639564	1.468839	0.000000
12	1	0	0.329703	1.981816	0.000000
13	1	0	2.800187	2.359441	0.000000
14	1	0	4.327543	0.418332	0.000000
15	1	0	3.426175	-1.881111	0.000000
16	1	0	0.970195	-2.248268	0.000000

***s-trans*-TS1**

Center Number	Atomic Number	Atomic Type	Coordinates (Angstroms) X	Y	Z
1	6	0	-0.905533	-0.085969	-0.000001
2	7	0	0.500679	-0.237355	-0.000002
3	6	0	-1.671048	-1.241845	0.000000
4	6	0	-3.049947	-1.111142	0.000000
5	6	0	-3.625882	0.152814	0.000001
6	7	0	1.465890	0.348946	-0.000003
7	7	0	3.001732	-0.911111	-0.000001
8	6	0	-2.834925	1.298853	0.000000
9	6	0	-1.456738	1.191833	0.000000
10	7	0	3.889264	-0.115761	0.000001
11	7	0	4.705264	0.684559	0.000003
12	1	0	-1.188012	-2.208160	-0.000001
13	1	0	-3.672104	-1.994330	0.000001
14	1	0	-4.702761	0.249693	0.000002
15	1	0	-3.294160	2.277064	0.000001
16	1	0	-0.818319	2.063532	-0.000001

***s-cis*-TS2**

Center Number	Atomic Number	Atomic Type	Coordinates (Angstroms) X	Y	Z
1	6	0	0.000000	0.624432	0.000000
2	7	0	0.182788	-0.781907	0.000000
3	6	0	1.164884	1.385511	0.000000
4	6	0	1.092282	2.771143	0.000000
5	6	0	-0.143295	3.403283	0.000000
6	7	0	-0.858698	-1.462269	0.000000
7	7	0	-0.835235	-2.735308	0.000000
8	6	0	-1.307257	2.640151	0.000000
9	6	0	-1.243771	1.256662	0.000000
10	7	0	0.568748	-3.220368	0.000000
11	7	0	1.388771	-3.942479	0.000000
12	1	0	2.119537	0.876375	0.000000
13	1	0	2.002423	3.355674	0.000000
14	1	0	-0.202613	4.483056	0.000000
15	1	0	-2.272631	3.128698	0.000000
16	1	0	-2.148395	0.665425	0.000000

***s-trans*-TS2**

Center Number	Atomic Number	Atomic Type	Coordinates (Angstroms) X	Y	Z
1	6	0	0.000000	0.928192	0.000000
2	7	0	-1.179476	0.138344	0.000000
3	6	0	-0.200821	2.305885	0.000000
4	6	0	0.882887	3.172513	0.000000
5	6	0	2.177171	2.670376	0.000000
6	7	0	-0.942189	-1.101200	0.000000
7	7	0	-1.913353	-1.887368	0.000000
8	6	0	2.377796	1.293454	0.000000
9	6	0	1.300545	0.422167	0.000000
10	7	0	-1.288084	-3.407273	0.000000
11	7	0	-1.333405	-4.495393	0.000000
12	1	0	-1.215386	2.682039	0.000000
13	1	0	0.713965	4.241048	0.000000
14	1	0	3.023972	3.342956	0.000000
15	1	0	3.383894	0.895189	0.000000
16	1	0	1.463629	-0.646519	0.000000

TSrot

Center Number	Atomic Number	Atomic Type	Coordinates (Angstroms) X	Y	Z
1	6	0	-1.243337	-1.128191	0.041795
2	6	0	-0.690398	0.129990	-0.192371
3	6	0	-1.480983	1.271192	-0.180530
4	6	0	-2.841119	1.161615	0.073014
5	6	0	-3.399200	-0.086399	0.307503
6	6	0	-2.600176	-1.227953	0.290298
7	7	0	0.693928	0.358609	-0.466503
8	7	0	1.402544	-0.630417	-0.423484
9	7	0	2.779175	-0.290302	-0.789538
10	7	0	3.400652	0.073888	0.210261
11	7	0	4.027776	0.400122	1.076068
12	1	0	-1.018215	2.230388	-0.369135
13	1	0	-3.460621	2.047498	0.084156
14	1	0	-4.459220	-0.175905	0.502830
15	1	0	-3.041945	-2.198444	0.470514
16	1	0	-0.617240	-2.008365	0.025766

TSsn2

Center Number	Atomic Number	Atomic Type	Coordinates (Angstroms) X	Y	Z
1	6	0	0.295376	-0.359268	-0.079997
2	7	0	-1.076378	-1.127576	-0.833783

3	6	0	1.225987	-1.222272	0.436492
4	6	0	2.522597	-0.726434	0.490833
5	6	0	2.827133	0.537056	-0.004851
6	7	0	-2.017993	-0.936643	-1.359398
7	6	0	1.833017	1.323770	-0.567972
8	6	0	0.517757	0.870352	-0.639901
9	1	0	0.959225	-2.200542	0.804733
10	1	0	3.297139	-1.349303	0.916437
11	1	0	3.843955	0.899840	0.033528
12	1	0	2.063397	2.302337	-0.966304
13	1	0	-0.279196	1.461090	-1.071026
14	7	0	-2.093529	0.534846	0.876474
15	7	0	-1.253105	-0.052826	1.459115
16	7	0	-2.875527	1.060392	0.211164

TS1per

Center Number	Atomic Number	Atomic Type	Coordinates (Angstroms) X	Y	Z
1	7	0	1.278541	-2.757075	0.000000
2	7	0	0.249766	-3.218452	0.000000
3	7	0	-1.023970	-2.909626	0.000000
4	7	0	-1.061186	-1.522249	0.000000
5	7	0	-0.002183	-0.920968	0.000000
6	6	0	0.000000	0.498587	0.000000
7	6	0	1.250118	1.102508	0.000000
8	6	0	1.341244	2.486544	0.000000
9	6	0	0.186512	3.257050	0.000000
10	6	0	-1.062470	2.642881	0.000000
11	6	0	-1.165302	1.262591	0.000000
12	1	0	2.134522	0.479757	0.000000
13	1	0	2.312779	2.960954	0.000000
14	1	0	0.256394	4.336180	0.000000
15	1	0	-1.961042	3.244653	0.000000
16	1	0	-2.130050	0.776075	0.000000

TS2per

Center Number	Atomic Number	Atomic Type	Coordinates (Angstroms) X	Y	Z
1	6	0	0.408497	-0.016698	-0.163394
2	7	0	-0.993207	0.031457	-0.311051
3	6	0	1.102090	1.177826	-0.315999
4	6	0	2.477451	1.185560	-0.144152
5	6	0	3.154191	0.009397	0.153010
6	7	0	-1.766850	-0.965657	-0.430779

7	7	0	-2.925296	-0.936167	-0.157132
8	6	0	2.448448	-1.179328	0.291068
9	6	0	1.070004	-1.200329	0.147141
10	7	0	-3.054738	0.698943	0.464192
11	7	0	-2.011252	1.192115	0.427932
12	1	0	0.563166	2.081487	-0.564072
13	1	0	3.021364	2.113401	-0.255112
14	1	0	4.228306	0.017997	0.275135
15	1	0	2.970706	-2.097766	0.521345
16	1	0	0.511777	-2.118527	0.264522

Full reference 18

Gaussian 09, Revision B.01, M. J. Frisch, G. W. Trucks, H. B. Schlegel, G. E. Scuseria, M. A. Robb, J. R. Cheeseman, G. Scalmani, V. Barone, B. Mennucci, G. A. Petersson, H. Nakatsuji, M. Caricato, X. Li, H. P. Hratchian, A. F. Izmaylov, J. Bloino, G. Zheng, J. L. Sonnenberg, M. Hada, M. Ehara, K. Toyota, R. Fukuda, J. Hasegawa, M. Ishida, T. Nakajima, Y. Honda, O. Kitao, H. Nakai, T. Vreven, J. A. Montgomery, Jr., J. E. Peralta, F. Ogliaro, M. Bearpark, J. J. Heyd, E. Brothers, K. N. Kudin, V. N. Staroverov, T. Keith, R. Kobayashi, J. Normand, K. Raghavachari, A. Rendell, J. C. Burant, S. S. Iyengar, J. Tomasi, M. Cossi, N. Rega, J. M. Millam, M. Klene, J. E. Knox, J. B. Cross, V. Bakken, C. Adamo, J. Jaramillo, R. Gomperts, R. E. Stratmann, O. Yazyev, A. J. Austin, R. Cammi, C. Pomelli, J. W. Ochterski, R. L. Martin, K. Morokuma, V. G. Zakrzewski, G. A. Voth, P. Salvador, J. J. Dannenberg, S. Dapprich, A. D. Daniels, O. Farkas, J. B. Foresman, J. V. Ortiz, J. Cioslowski, and D. J. Fox, Gaussian, Inc., Wallingford CT, 2010.